

Run-up of dispersive and breaking waves on beaches

OCEANOLOGIA, 43 (1), 2001.
pp. 61–97.

© 2001, by Institute of
Oceanology PAS.

KEYWORDS

Surface waves
Run-up process
Sandy beaches
Filtration
Mathematical modelling

STANISŁAW R. MASSEL
Institute of Oceanology,
Polish Academy of Sciences,
Powstańców Warszawy 55, PL-81-712 Sopot, Poland;
e-mail: smas@iopan.gda.pl

EFIM N. PELINOVSKY
Institute of Applied Physics,
Russian Academy of Sciences,
Ulyanov 46, RU-603600 Nizhniy Novgorod, Russia;
e-mail: enpeli@appl.nnov.su

Manuscript received 18 December 2000, reviewed 8 February 2001, accepted 12 February 2001.

Abstract

Transformation of waves on sandy beaches, their breaking, set-up and run-up are the main factors contributing to fluctuations in the water table and groundwater flow. In this paper, the run-up mechanisms have been studied using analytical models. In contrast to the standard models, the waves approaching the shoreline are assumed to be dispersive and the equivalence of the non-linear and linear solutions for the extreme characteristics of wave run-up, such as the height of maximum run-up and the velocity of run-up, are used.

A linear system of equations for the run-up of breaking waves is developed. This system is based on the application of the mild-slope equation in the deeper area, where waves are dispersive, while the linear equations of shallow water are applied close to the shoreline, where the water depth is a linear function of distance. The dissipation factor in the shallow water equation has been formulated using its resemblance to the mild-slope equation for a non-permeable sea bottom. Application of the method is illustrated for various bottom profiles and wave characteristics, and theoretical results compared well with experimental data. These solutions of the run-up phenomena will assist future studies on wave-induced beach groundwater flow.

1. Introduction

This paper is the first of an intended series of papers on the dynamics of surface waves on a beach surface and on wave-induced fluctuations of the groundwater table. This work has been motivated by the research within the LITUS Project (Interaction of Biodiversity, Productivity and Tourism in European Sandy Beaches). The basic objectives of the Project are to assess the vulnerability of a sandy beach's biodiversity and the functioning of a beach ecosystem, as well as a better understanding of the interaction between tourism, natural changes, and physical marine factors of such an ecosystem. The LITUS Project provides a scientific, socio-economic and technological basis for understanding changes in European sandy beaches (Węśławski et al., in press).

Sandy beaches are highly exploited but very dynamic and fragile environments. The beach system is driven by the physical energy induced by waves and tides. The water flow through the beach body is of great importance in introducing water, organic materials and oxygen to the ground environment. It controls the vertical and horizontal, chemical and biological gradients, and nutrient exchange in the beach (McLachlan 1989). Further, water filtration through a sandy beach is considered to be significant for swash-backwash dynamics and accretion-erosion on the beach face (Turner 1995).

The measurements by McLachlan (1989) showed that the volume of water filtered through sandy beaches depends on the beach type. In general, beaches can be classified as reflective, intermediate, or dissipative (Short 1991). For tideless seas, such as the Baltic, the basic dimensionless beach classification parameter Ω has the form

$$\Omega = \frac{\bar{H}_{br}}{wT}, \quad (1)$$

where \bar{H}_{br} is the mean breaker height, w is the mean fall velocity, and T is the wave period. Assuming that the typical storm wave parameters are $\bar{H}_{br} \approx 1$ m and $T = 6$ s, and the median size of sand $D_{50} \approx 0.3$ mm, the fall velocity in eq. (1) becomes $w = 0.0246$ m s⁻¹ (SPM 1984). The resulting value of the dimensionless parameter $\Omega \approx 6.8$ indicates that the beach under consideration is of the dissipative type. McLachlan (1989) showed that dissipative beaches filter low volumes of seawater. However, during strong storms, the filtered volume can increase by one order of magnitude.

Wave motion on beaches is very complex and the groundwater flow is different in different beach regions. In Region 3, between points D and E (see Fig. 1), the wave run-up infiltration contributes mainly to the raising of the coastal water table. The hypothetical distribution of the infiltration velocity U_f induced by the run-up is shown in the same figure, and the

vertical axis $n_i N^{-1}$ denotes the ratio of the events when the beach surface is covered by water to the total number of events. The wave run-up infiltration process, under the Dupuit-Forchheimer assumption, obeys the Boussinesq equation. When there is no sink or source landward of the run-up limit, the water table is horizontal landward of the run-up limit (Li & Barry 2000).

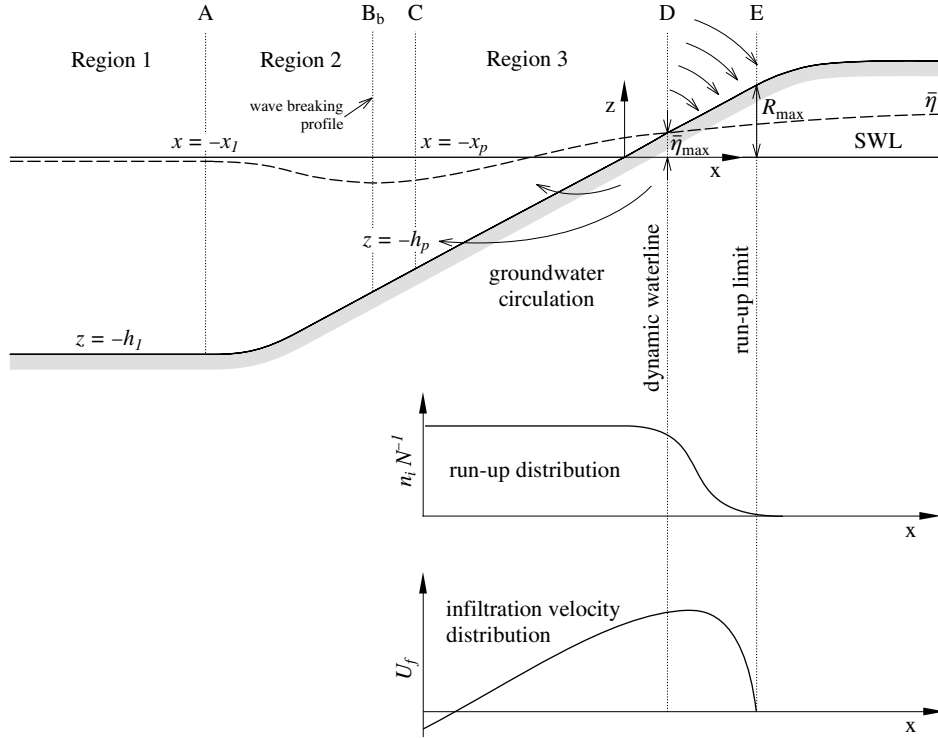


Fig. 1. Reference scheme and relationships between wave run-up, infiltration and coastal watertable

The beach groundwater flow in the set-up region, between points B_b and D (see Fig. 1), induces a groundwater circulation which contributes to the submarine groundwater discharge (Kang & Nielsen 1996, Li & Barry 2000). Little is known about the groundwater flow in this region. One of the models of the groundwater flow is the Longuet-Higgins (1983) analytical solution for the circulation induced by wave set-up. The problem was solved for a semi-infinite domain, but the free surface boundary conditions at the water table and the landward boundaries were not included in the solution.

For tideless seas, the groundwater flow is totally controlled by the dynamics of surface waves on the beach. As waves propagate towards the shore, they become steeper owing to the shallowing of water depth, and

at some depth they lose their stability and finally start to break. When waves break, wave energy is dissipated and the radiation stress is reduced. Longuet-Higgins & Stewart (1964) proved that shoaling, refraction and dissipation processes induce spatial changes in the radiation stress, which give rise to changes in the mean sea level (MSL). The balance of the sea level gradient and the gradient of radiation stress takes the form

$$\frac{dS_{xx}}{dx} + \rho g (h + \bar{\eta}) \frac{d\bar{\eta}}{dx} = 0, \quad (2)$$

in which $\bar{\eta}$ is the change of MSL due to wave action, and S_{xx} is the radiation stress tensor component. The change of $\bar{\eta}$ due to wave action is shown in Fig. 1. The maximum set-down appears close to breaking point (point B_b), while the maximum set-up $\bar{\eta}_{\max}$ occurs at point D.

The wave run-up height R_{\max} is defined here as the maximum vertical height above still water level reached by the wave uprush (point E in Fig. 1). The run-up height is always greater than the wave set-up. On the other hand, wave run-down is defined as the lowest vertical height reached by the backwash of a wave before the uprush of the next wave commences to run-up the beach face.

There is a considerable literature on the estimation of maximum run-up on beaches and engineering structures. In particular, experimental studies on wave run-up for periodic waves were reported by Saville (1958), Savage (1958), Hunt (1959), Battjes (1974), Kobayashi & Greenwald (1986), Walton & Ahrens (1989) and Gourlay (1992). In all these studies, the so-called Iribarren number or surf parameter was used for data presentation (see Section 2 for more details). This approach yields the values of the possible maximum wave run-up limit, which is very valuable engineering information, but provides no information on the dynamics of run-up, namely on the position of the water surface on the slope, the movement velocity of the waterline and the time of water residence on the particular beach segments, which are of great importance for the evaluation of groundwater flow.

On the other hand, in coastal oceanography, run-up is considered a basic mechanism determining the impact of tsunami waves on a coast. Tsunami waves belong to the class of very long waves and are usually modelled through the solitary wave representation (Mazova & Pelinovsky 1982, Kaystrenko et al. 1985, Titov & Synolakis 1995).

The wave run-up limit and induced water infiltration into a beach body is a response to the instantaneous flow of the surface water. Therefore, modelling the surface oscillation should be based on the phase-resolving wave type model. The key element of the model proposed in this paper is the proper representation of the wave run-up mechanism for the incident dispersive waves. It should be noted that available run-up models usually

assume that waves are non-dispersive and that the phase velocity depends on the water depth only (Carrier & Greenspan 1958, Carrier 1966, Le Mehaute et al. 1968, Pelinovsky 1982, Voltzinger et al. 1989, Pelinovsky & Mazova 1992). This assumption is applicable to tsunami and wind-induced waves very close to the shoreline. However, in deeper water, waves are usually dispersive. Thus, we need an approach in which the dispersive character of waves is maintained seawards and the approximation of shallow water is used close to the waterline. The possibility of developing such a combined model of the run-up of dispersive waves on a beach was mentioned in another paper by the authors (Massel et al. 1990). However, in that paper, the transformation of the deep water waves to the shallow water was represented in a very approximate way using the linear wave theory. Moreover, energy dissipation due to wave breaking was totally neglected.

In this paper an attempt is made to develop a more complex approach for the run-up of dispersive breaking and non-breaking waves. Waves approaching the shallow water area are modelled by the mild-slope equation (Berkhoff 1973, Massel 1996, 1999). At very small water depths, the non-linear and linear equations for shallow water waves are considered and the dissipation due to wave breaking is included, providing a more realistic estimation of run-up characteristics. However, the permeability of the sea bottom is neglected and analytical methods are preferred to a purely numerical approach.

The paper is organised as follows. The governing equations for Regions 1 and 2 are given in Section 2. The non-linear and linear equations of the wave motion in Region 3, as well as the dissipation terms are discussed in Section 3. The solution of the boundary value problem is given in Section 4. Section 5 contains examples of numerical calculations and comparison with experiments, while the main conclusions are listed in Section 6.

2. Governing equations for wave motion in Regions 1 and 2

Consider the coordinate system $0(x, y, z)$ with the z -axis positive upwards and equal to zero at the still water level (Fig. 1). To facilitate the analysis, the whole area of interest is divided into regions in which the governing equations are established. The solutions in particular regions are matched using the conditions of continuity of the pressure and velocities. We assume that the water is incompressible, the sea bottom is non-permeable, and that a monochromatic wave train of a given frequency ω and wave height H_i is normally incident on the beach. In Region 1 ($-\infty < x \leq -x_1$), the water depth is assumed constant and equal to h_1 . In Region 2 ($-x_1 < x \leq -x_p$), the water depth is an arbitrary function of the distance x ,

while in Region 3 ($-x_p < x < \infty$), the water depth is a linear function of x , i.e.

$$h(x) = -\beta x, \quad (3)$$

in which β is the beach slope.

Region 1 ($-\infty < x \leq -x_1; z = h_1$)

In this Region, the wave field consists of the incident and reflected waves, and the potential Φ_1 takes the form (Massel 1989)

$$\begin{aligned} \Phi_1(x, z, t) &= \frac{-igH_i}{2\omega} Z_1(z) \{ \exp[ik_1(x + x_1)] + \\ &+ K_R \exp[-ik_1(x + x_1)] \} \exp(-i\omega t), \end{aligned} \quad (4)$$

in which

$$Z_1(z) = \frac{\cosh k_1(z + h_1)}{\cosh k_1 h_1}, \quad (5)$$

K_R is the unknown complex reflection coefficient, and wave number k_1 should satisfy the dispersion relation

$$\omega^2 = gk_1 \tanh(k_1 h_1). \quad (6)$$

Region 2 ($-x_1 < x \leq -x_p; -h_1 \leq z \leq -h_p$)

In Region 2, the water depth $h(x)$ can vary substantially, and the refraction and diffraction effects cannot be neglected. In order to account for these effects an approach based on the mild-slope equation (Berkhoff 1973) is used. When the dissipation due to breaking is included, the governing velocity potential $\Phi_2(x, z, t)$ can be represented in the form (Massel 1996, Massel & Gourlay 2000)

$$\Phi_2(x, y, z, t) = \frac{-igH_i}{2\omega} Z_2(z) \varphi_2(x) \exp(-i\omega t), \quad (7)$$

in which

$$Z_2(z) = \frac{\cosh k_2(z + h_2)}{\cosh k_2 h_2}, \quad (8)$$

and

$$\frac{d^2 \varphi_2}{dx^2} + (CC_g)^{-1} \frac{dCC_g}{dx} \frac{d\varphi_2}{dx} + (k_2^2 + i\gamma k_2) \varphi_2 = 0. \quad (9)$$

The $\varphi_2(x)$ function is the non-dimensional wave height $H(x)/H_i$; C and C_g are the respective phase and group velocities, and wave number k_2 satisfies the dispersion relation

$$\omega^2 = gk_2 \tanh(k_2 h_2). \quad (10)$$

In the case of a steeper bottom, more elaborate wave models should be used (see for example Massel 1993, Athanassoulis & Belibassakis 1999).

The unknown damping factor γ in eq. (9) consists of two components, i.e. the dissipation due to wave breaking γ_b and that due to bottom friction γ_f (Massel 1996)

$$\gamma = \gamma_b + \gamma_f, \quad (11)$$

in which

$$\gamma_b = \frac{8 \langle \epsilon_b \rangle}{\rho g C_g H^2}, \quad (12)$$

$$\gamma_f = \frac{8 \langle \epsilon_f \rangle}{\rho g C_g H^2}, \quad (13)$$

where $\langle \epsilon_b \rangle$ and $\langle \epsilon_f \rangle$ represent the average rate of energy dissipation (per unit area) due to wave breaking and bottom friction respectively. In the shallow water zone the dissipation due to wave breaking is substantially greater than that due to bottom friction. This friction is therefore omitted in the following analysis. Wave breaking is a highly non-linear process and at present there is no theoretical solution to this problem. However, there is a wide body of literature aimed at the parameterisation of the breaking process. In particular, the periodic bore model of Battjes & Janssen (1978) is used in this paper to account for the rate of energy dissipation, and the damping factor γ_b becomes (Massel & Belberova 1990, Massel & Gourlay 2000)

$$\gamma_b = \frac{\alpha \omega \sqrt{gh} H}{\pi C C_g h}, \quad (14)$$

in which α is an experimental parameter of the order of one, and the wave height H is given by

$$H = H_i \sqrt{[\Re \varphi_2(x)]^2 + [\Im \varphi_2(x)]^2}, \quad (15)$$

in which \Re and \Im are the real and imaginary parts of the complex function φ_2 .

The initiation of energy dissipation or the extent of the surf zone, in which equation (2.9) should be used, is controlled by the non-dimensional maximum allowable wave height $\left(\frac{H_m}{h}\right)$. In this paper the formula proposed by Singamsetti & Wind (1980) is applied:

$$\frac{H_m}{h} = 0.937 \left| \frac{dh}{dx} \right|^{0.155} \left(\frac{H_0}{L_0} \right)^{-0.130}, \quad (16)$$

where H_0 and L_0 are the deep water wave height and length respectively.

The wave height attenuation in Region 2 should be supplemented by the estimation of the wave induced set-up and set-down (see eq. (2)). If we

neglect the reflected waves and introduce the wave energy E for progressive waves, the tensor S_{xx} takes the form (Massel 1989)

$$S_{xx} = E \left(2m - \frac{1}{2} \right), \quad (17)$$

where

$$E = \frac{1}{8} \rho g H^2 \quad (18)$$

and

$$m = \frac{1}{2} \left(1 + \frac{2kh}{\sin 2kh} \right). \quad (19)$$

For a gentle bottom slope, the resulting gradient of radiation stress is affected only by the local gradient of wave height

$$\frac{dS_{xx}}{dx} = \frac{1}{8} \rho g R(x), \quad (20)$$

in which

$$R(x) = \frac{\partial S_{xx}}{\partial H} \frac{dH}{dx} = \frac{(4m-1)}{8} H \frac{dH}{dx} \quad (21)$$

After substituting eq. (20) into eq. (2) we obtain

$$\frac{d\bar{\eta}}{dx} = \frac{-1}{8(h+\bar{\eta})} R(x) = -\frac{(4m-1)}{8} \frac{H}{h} \frac{dH}{dx}. \quad (22)$$

Eqs. (9) and (22) form a final set of equations for the unknown non-dimensional wave height φ and set-up $\bar{\eta}$. This set of equations is solved in a recurrent manner, i.e. first the non-dimensional wave height φ is determined for $\bar{\eta} = 0$, then the set-up $\bar{\eta}$ is established and a new water depth ($h + \bar{\eta}$) is used in the calculation of a new value of φ . The process is repeated until the required accuracy is obtained. In this paper Cholesky's method (Haggerty 1972) was used for solving eq. (9) and a predictor-corrector method was applied to eq. (22).

3. Governing equations for wave motion in Region 3

3.1. Non-linear formulation of the problem

In Region 3, close to the shoreline, the water depth is very small. Therefore, wave motion can be described by the non-linear equations of shallow water (Kaystrenko et al. 1985, Massel 1989)

$$\left. \begin{aligned} \frac{\partial \bar{u}}{\partial t} + \bar{u} \frac{\partial \bar{u}}{\partial x} + g \frac{\partial \zeta}{\partial x} &= 0 \\ \frac{\partial \zeta}{\partial t} + \frac{\partial}{\partial x} [(h + \zeta) \bar{u}] &= 0 \end{aligned} \right\}, \quad (23)$$

where ζ is the surface elevation, \bar{u} is the horizontal flow velocity (averaged over the water depth) and the water depth h satisfies eq. (3).

In order to define the relative importance of the particular terms in eqs. (23), the following non-dimensional variables are introduced:

$$\tilde{t} = \omega t, \quad \tilde{x} = \frac{\beta x}{H_i}, \quad \tilde{\zeta} = \frac{\zeta}{H_i} \quad \text{and} \quad \tilde{u} = \frac{\beta \bar{u}}{H_i \omega}. \quad (24)$$

Using the variables (24) into (23) we obtain

$$\left. \begin{aligned} \frac{\partial \tilde{u}}{\partial \tilde{t}} + \tilde{u} \frac{\partial \tilde{u}}{\partial \tilde{x}} + \frac{1}{B_r} \frac{\partial \tilde{\zeta}}{\partial \tilde{x}} &= 0 \\ \frac{\partial \tilde{\zeta}}{\partial \tilde{t}} + \frac{\partial}{\partial \tilde{x}} [(-\tilde{x} + \tilde{\zeta}) \tilde{u}] &= 0 \end{aligned} \right\}, \quad (25)$$

where

$$B_r = \frac{H_i \omega^2}{g \beta^2}. \quad (26)$$

Eqs. (25) indicate that the run-up of waves on a plane beach is controlled by one non-dimensional similarity parameter only, which is of great importance for the modelling procedure.

To clarify the physical meaning of the parameter B_r , eq. (26) is rewritten as

$$\frac{1}{B_r} = \frac{g \beta^2}{H_i \omega^2} = \frac{1}{2\pi} \left(\frac{\beta}{\sqrt{\frac{H_i}{L_0}}} \right)^2 = \frac{1}{2\pi} (\xi_0)^2, \quad (27)$$

or

$$B_r = \frac{2\pi}{\xi_0^2}, \quad (28)$$

where

$$\xi_0 = \frac{\beta}{\sqrt{\frac{H_i}{L_0}}}, \quad (29)$$

and $L_0 = 2\pi g/\omega^2$ is the wavelength in deep water. When the wave height H_i is approximately equal to the wave height in deep water, i.e. $H_i \approx H_0$, the parameter ξ_0 becomes exactly equal to the surf parameter introduced by Battjes (1974). The parameter ξ_0 can be used to classify various types of breaker into three main categories (Battjes 1974, Massel 1989)

$$\begin{aligned} \text{surging and collapsing} & \text{ if } & 3.3 < \xi_0, \\ \text{plunging} & \text{ if } & 0.5 < \xi_0 < 3.3, \\ \text{spilling} & \text{ if } & \xi_0 < 0.5. \end{aligned}$$

Using eq. (28), the corresponding classification in terms of parameter B_r yields

$$\begin{array}{ll} \text{surging and collapsing} & \text{if } B_r < 0.58, \\ \text{plunging} & \text{if } 0.58 < B_r < 25.0, \\ \text{spilling} & \text{if } B_r > 25.0. \end{array}$$

It should be noted that the range of variability of parameter B_r is much larger than the corresponding range for parameter ξ_0 . Therefore, the parameter ξ_0 is better defined and the particular type of breaking is classified with greater accuracy.

The solution of eqs. (23) can be found using the method developed by Carrier & Greenspan (1958). In this method, eqs. (23) are rewritten in a form in which some characteristic variables σ and λ act as independent variables, and variables u, ζ, x and t are the unknown functions of σ and λ . Following Voltzinger et al. (1989), we define σ and λ as follows:

$$\left. \begin{array}{l} \lambda = \bar{u} + g\beta t, \\ \sigma = 2\sqrt{g(\zeta - \beta x)} \end{array} \right\}. \quad (30)$$

Additional simplification is obtained when the potential $\psi(\sigma, \lambda)$ is introduced:

$$\bar{u} = \frac{1}{\sigma} \frac{\partial \psi(\sigma, \lambda)}{\partial \sigma}. \quad (31)$$

The details of the transformation from variables (x, t) into (σ, λ) can be found elsewhere (Carrier & Greenspan 1958, Kaystrenko et al. 1985, Voltzinger et al. 1989) and are not repeated here. The final relationships between x, t, ζ and σ, λ, ψ become

$$\zeta = \frac{1}{2g} \left(\frac{\partial \psi}{\partial \lambda} - \bar{u}^2 \right), \quad (32)$$

$$x = \frac{1}{2g\beta} \left(\frac{\partial \psi}{\partial \lambda} - \bar{u}^2 - \frac{\sigma^2}{2} \right), \quad (33)$$

$$t = \frac{\lambda - \bar{u}}{g\beta}. \quad (34)$$

Using formulas (31)–(34), the initial non-linear set of eqs. (23) can be reduced to the linear equation for the potential $\psi(\sigma, \lambda)$

$$\frac{\partial^2 \psi(\sigma, \lambda)}{\partial \lambda^2} - \frac{\partial^2 \psi(\sigma, \lambda)}{\partial \sigma^2} - \frac{1}{\sigma} \frac{\partial \psi(\sigma, \lambda)}{\partial \sigma} = 0. \quad (35)$$

From eq. (30) it follows that the value $\sigma = 0$ corresponds to the moving shoreward boundary, therefore the solution of eq. (35) can be considered in the fixed σ space: $0 < \sigma < \infty$. The method of separating the variables gives

$$\psi(\sigma, \lambda) = AJ_0(l\sigma) \sin(l\lambda), \quad (36)$$

where $J_0(l\sigma)$ is the Bessel function of the first kind and of zero order. The constants A and l should be defined from the matching conditions at the seaward and shoreward boundaries of Region 3.

3.2. Boundary conditions for Region 3

At the seaward boundary of Region 3, i.e. at $x = -x_p$ (see Fig. 1), the wave amplitude should be equal to the amplitude of the linear wave in Region 2. This condition is satisfied only when $\sigma \gg 1$ for $x = -x_p$. Then eqs. (31)–(34) yield

$$\zeta = \frac{1}{2g} \frac{\partial \psi}{\partial \lambda}, \quad x = -\frac{\sigma^2}{4g\beta}, \quad t = \frac{\lambda}{g\beta}. \quad (37)$$

Using the asymptotic form of the Bessel function $J_0(l\sigma)$ for large arguments (Abramowitz & Stegun 1975), i.e.

$$J_0(l\sigma) \approx \sqrt{\frac{2}{\pi l\sigma}} \cos\left(l\sigma - \frac{\pi}{4}\right) \text{ for } \sigma \gg 1, \quad (38)$$

we obtain the surface ordinate ζ in the form

$$\zeta(\sigma, \lambda) = \frac{Al}{2g} J_0(l\sigma) \cos(l\lambda) \approx \frac{A}{g} \sqrt{\frac{l}{2\pi\sigma}} \cos(l\lambda) \cos\left(l\sigma - \frac{\pi}{4}\right), \quad (39)$$

or

$$\zeta(\sigma, \lambda) \approx \frac{A}{2g} \sqrt{\frac{l}{2\pi\sigma}} \left\{ \cos\left[l(\sigma + \lambda) - \frac{\pi}{4}\right] + \cos\left[l(\sigma - \lambda) - \frac{\pi}{4}\right] \right\}. \quad (40)$$

To define parameters A and l we use the fact that at the seaward boundary of Region 3 ($x = -x_p$) waves are periodic with frequency ω and height H_p , i.e.

$$lg\beta = \omega \text{ or } l = \frac{\omega}{g\beta}, \quad (41)$$

and

$$\frac{A}{g} \sqrt{\frac{l}{2\pi\sigma}} = \frac{H_p}{2} \quad (42)$$

or

$$A = \sqrt{\pi} \left(\frac{\beta^3 g^7 x_p}{\omega^2} \right)^{1/4} H_p. \quad (43)$$

Substituting eqs. (30), (34) and (43) into eq. (40) gives

$$\begin{aligned} \zeta(x, t) \approx & \frac{H_p}{2} \left| \frac{x}{x_p} \right|^{-1/4} \left\{ \cos\left[2\omega \left(\frac{|x|}{g\beta}\right)^{1/2} + \omega t - \frac{\pi}{4}\right] + \right. \\ & \left. + \cos\left[2\omega \left(\frac{|x|}{g\beta}\right)^{1/2} - \omega t - \frac{\pi}{4}\right] \right\}. \end{aligned} \quad (44)$$

Eq. (44) describes the wave travelling shoreward from the region of large negative x , and the reflected wave travels out to sea. For non-dissipative motion, the reflection coefficient becomes unity and far out at sea the wave is periodic in time and space. Assuming a plane beach, we have $\left|\frac{x}{x_p}\right| = \left|\frac{h}{h_p}\right|$. Then eq. (44) indicates that the amplitude in shallow water attenuates according to Green's law (Massel 1989).

The other limiting value, $\sigma = 0$, corresponds to the moving shoreward boundary which determines the run-up distance on the beach and the run-up time. Eqs. (33), (34) and (36) give

$$x = \frac{1}{2g\beta} \left[Al \cos(l\lambda) - \frac{A^2 l^4}{4} \sin^2(l\lambda) \right] \quad (45)$$

and

$$t = \frac{1}{g\beta} \left[\lambda + \frac{Al^2}{2} \sin(l\lambda) \right]. \quad (46)$$

Therefore, the maximum and minimum run-up distances on the beach are

$$x_{\max} = \frac{1}{2} \sqrt{\frac{\pi\omega}{g}} \beta^{-5/4} (g|x_p|)^{1/4} H_p \quad (47)$$

and

$$x_{\min} = -\frac{1}{2} \sqrt{\frac{\pi\omega}{g}} \beta^{-5/4} (g|x_p|)^{1/4} H_p. \quad (48)$$

Eq. (47) implies that on a plane beach, the height of the maximum run-up R_{\max} becomes

$$\frac{R_{\max}}{H_p} = \frac{1}{2} \left(\frac{\pi\omega}{\beta} \sqrt{\frac{h_p}{g}} \right)^{1/2}. \quad (49)$$

The maximum run-up R_{\max} is defined here as the vertical distance from the maximum wave surface extent on the beach, measured from the SWL, when the set-up is not taken into account. It should be noted that the level of the run-down is equal to that of the run-up.

The corresponding velocity of the shoreward boundary motion becomes

$$\bar{u}_b = \lim_{\sigma \rightarrow 0} \left(\frac{1}{\sigma} \frac{\partial \psi}{\partial \sigma} \right) = -\frac{Al^2}{2} \sin(l\lambda), \quad (50)$$

or

$$\bar{u}_b = -\frac{\omega}{2\beta} \left(\frac{\pi\omega}{\beta} \sqrt{\frac{h_p}{g}} \right)^{1/2} H_p \sin(l\lambda). \quad (51)$$

To illustrate the above relationships, the variation of the shoreline distance against the initial waterline position, $x = 0$, and the velocity of the shoreline movement are shown in Fig. 2a for $H_p = 0.5$ m, $T = 12$ s, $h_p = 10$ m, $\beta = 0.2$ and $x_p = 50$. Fig. 2b shows the percentage of beach face coverage by water.

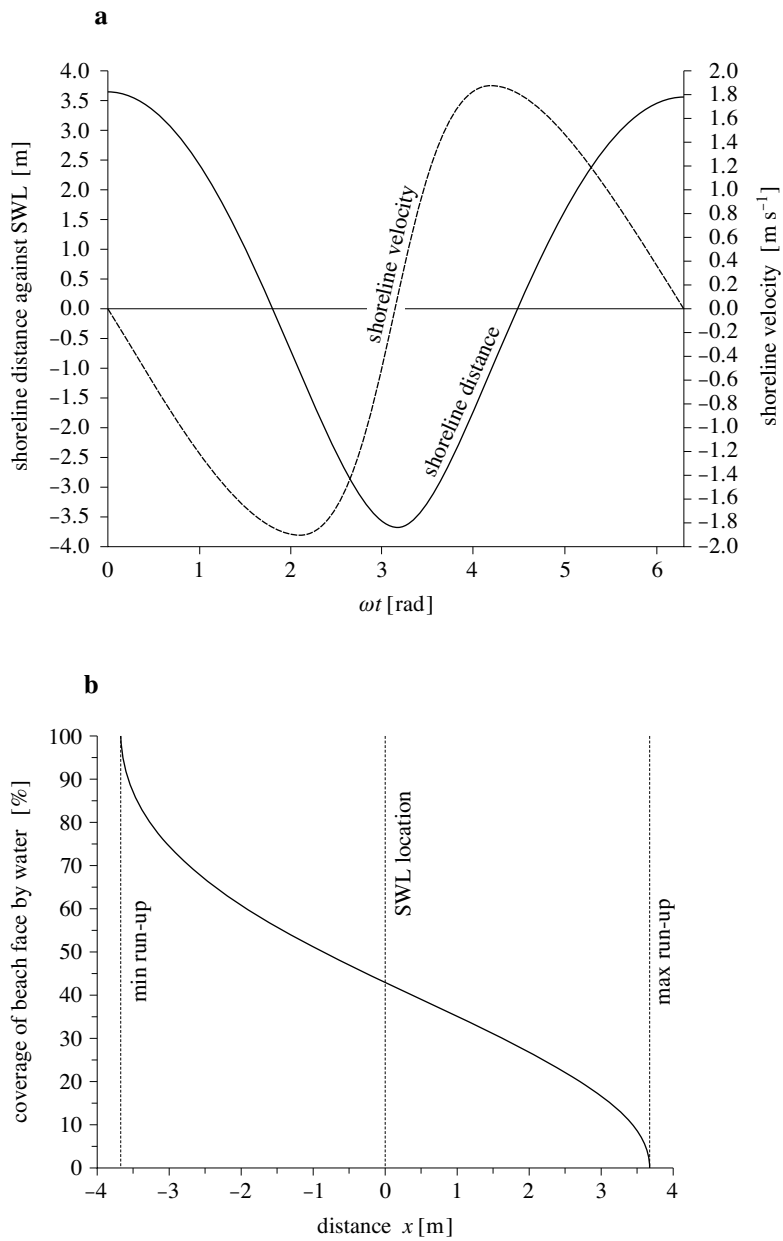


Fig. 2. Wave run-up on a plane beach: variation of shoreline distance and velocity of shoreline movement as a function of time (a), percentage of coverage of beach face during run-up (b)

The lower limit of the run-up is always covered by water, while the coverage of the upper limit by water becomes zero.

At the end of this Section, we note that the relationships of the variables (σ, λ) and (x, t) are not explicit. Therefore, the determination of the run-up level for an arbitrary location and time can only be done numerically. Examples of such calculations are given by Carrier & Greenspan (1958), Voltzinger et al. (1989) and others, and are not repeated here.

3.3. Equivalence of the non-linear and linear solutions for the extreme characteristics of wave run-up

Prior to deriving the solution for the run-up of breaking waves, we discuss the relationships between the non-linear and linear theory of run-up of non-breaking waves. For our starting point we use the linear version of the Carrier & Greenspan transformation in the form

$$\bar{u} = \frac{1}{\sigma_0} \frac{\partial \psi_0(\sigma_0, \lambda_0)}{\partial \sigma_0}, \quad (52)$$

$$\zeta = \frac{1}{2g} \left(\frac{\partial \psi_0}{\partial \lambda_0} \right), \quad (53)$$

$$x = -\frac{\sigma_0^2}{4g\beta}, \quad (54)$$

$$t = \frac{\lambda_0}{g\beta}, \quad (55)$$

and the linear approximation of the incident non-linear equations of shallow water:

$$\left. \begin{aligned} \frac{\partial \bar{u}}{\partial t} + g \frac{\partial \zeta}{\partial x} &= 0 \\ \frac{\partial \zeta}{\partial t} + \frac{\partial}{\partial x}(h\bar{u}) &= 0 \end{aligned} \right\}. \quad (56)$$

Substituting eqs. (52)–(55) into eq. (56) we obtain

$$\frac{\partial^2 \psi_0(\sigma_0, \lambda_0)}{\partial \lambda_0^2} - \frac{\partial^2 \psi_0(\sigma_0, \lambda_0)}{\partial \sigma_0^2} - \frac{1}{\sigma_0} \frac{\partial \psi_0(\sigma_0, \lambda_0)}{\partial \sigma_0}. \quad (57)$$

Comparison of eqs. (35) and (57) indicates that the resulting equation for the linear potential $\psi_0(\sigma_0, \lambda_0)$ is identical to the equation for the non-linear potential $\psi(\sigma, \lambda)$. Therefore, we can say that the values of functions $\psi(\sigma, \lambda)$ and $\psi_0(\sigma_0, \lambda_0)$, and especially their maxima, are identical. Moreover, very far from the waterline, $\sigma_0 \rightarrow \sigma$ and $\lambda_0 \rightarrow \lambda$, and both asymptotes of ψ and ψ_0 are the same and correspond to the same waves incident from Region 2. However, the function $\zeta(0, \lambda)$ resulting from the non-linear solution corresponds to the motion of the waterline, where $\zeta(0, \lambda) = R_{\max}$ and $x_{\max} = \frac{R_{\max}}{\beta}$. On the other hand, function $\zeta(0, \lambda_0)$ describes the oscillations of the surface elevation at the constant position of the waterline ($\sigma_0 = 0 \rightarrow x = 0$, see eq. (54)).

The above equivalence yields an important conclusion in that the maximum sea level at $x = 0$, resulting from the linear theory, is identical to the maximum run-up predicted by the non-linear theory. To be more specific, let us write the solution of eq. (57) in the form

$$\psi_0(\sigma_0, \lambda_0) = AJ_0(l\sigma_0) \sin(l\lambda_0), \quad (58)$$

and the surface elevation at $x = 0$ as

$$\zeta(0, \lambda_0) = \frac{1}{2g} \left(\frac{\partial \psi_0}{\partial \lambda_0} \right) = \frac{Al}{2g} \sin(l\lambda_0). \quad (59)$$

Therefore, the maximum of the elevation becomes

$$\max \{ \zeta(0, \lambda_0) \} = \frac{Al}{2g}. \quad (60)$$

On the other hand, from the non-linear theory we have (see eqs. (32) and (36))

$$\zeta(0, \lambda) = \frac{1}{2g} \left(\frac{\partial \psi(0, \lambda)}{\partial \lambda} - \bar{u}^2 \right) = \frac{1}{2g} \left(\frac{\partial \psi(0, \lambda)}{\partial \lambda} \right) = \frac{Al}{2g} \sin(l\lambda), \quad (61)$$

and

$$\max \{ \zeta(0, \lambda) \} = \frac{Al}{2g}. \quad (62)$$

Both maximum surface elevations are the same, although they appear at different locations. The first one appears at the constant point $x = 0$, while the second one corresponds to the most shoreward position of the dynamic waterline. Therefore, in order to find the exact maximum run-up height, it is sufficient to solve the linear system of equations and calculate the sea level at $x = 0$. We can also determine the exact velocity of the moving waterline by calculating the linear velocity at $x = 0$, i.e. for $\sigma_0 = 0$. However, it should be pointed out that within the linear approach it is not possible to determine the dynamics of the moving boundary. In the next Section we apply the above equivalence to predict the wave run-up on various types of beaches and to study the influence of wave breaking on the run-up height.

3.4. Influence of wave breaking on run-up in Region 3

Carrier & Greenspan's transformation is valid when the Jacobian of the transformation $J = \partial(x, t)/\partial(\sigma, \lambda) \neq 0$ for $\sigma > 0$ (Carrier & Greenspan 1958). This condition is satisfied when

$$\frac{R_{\max} \omega^2}{g\beta^2} = \tilde{B}_r < 1, \quad (63)$$

and the solution of eq. (35) represents waves which do not break. If the Jacobian does vanish for $\sigma > 0$, the waves must break. The critical parameter \tilde{B}_r is similar to the parameter B_r defined by eq. (26), but is

expressed in terms of the maximum run-up height. Both parameters are of the same order of magnitude. For typical values of wind induced waves and a gentle beach slope, i.e. when $\omega \approx 1 \text{ rad s}^{-1}$, $H_i = 1 \text{ m}$ and $\beta = 0.02$, we obtain $B_r = 250$. This value is much higher than the critical value $B_r \approx 1$. Therefore, the run-up of short wind induced waves is usually accompanied by wave breaking. To take into account wave breaking, the dissipative term should be included in the governing equations. However, an analytical non-linear solution of eqs. (23) including the dissipative factors cannot be obtained as the corresponding Carrier & Greenspan-type transformation for breaking waves does not exist. On the other hand, the equivalence of the maximum characteristics resulting from the linear and non-linear solutions, discussed in the above Section, suggests the use of the linear theory of shallow water to predict the run-up of breaking waves on the beach. Thus, consider a linear version of eqs. (23) with the dissipation term in the form (Dingemans 1997)

$$\left. \begin{aligned} \frac{\partial \bar{u}}{\partial t} + g \frac{\partial \zeta}{\partial x} + D_b \bar{u} &= 0 \\ \frac{\partial \zeta}{\partial t} + \frac{\partial}{\partial x} (h \bar{u}) &= 0 \end{aligned} \right\}, \quad (64)$$

where D_b is the dissipation factor due to wave breaking. As was mentioned above, the energy dissipation due to bottom friction is neglected. Combining both eqs. (64) we obtain

$$\frac{\partial^2 \bar{u}}{\partial t^2} - \frac{\partial}{\partial x} \left[\frac{\partial}{\partial x} (gh \bar{u}) \right] + D_b \frac{\partial \bar{u}}{\partial t} = 0. \quad (65)$$

Introduction of the velocity potential $\Phi_3(x, t)$

$$\bar{u} = \frac{\partial \Phi_3}{\partial x} \quad (66)$$

into eq. (65) yields

$$\frac{\partial^2 \Phi_3}{\partial t^2} - \frac{\partial}{\partial x} \left(gh \frac{\partial \Phi_3}{\partial x} \right) + D_b \frac{\partial \Phi_3}{\partial t} = 0. \quad (67)$$

As with the potentials in Regions 1 and 2, we represent $\Phi_3(x, t)$ as follows:

$$\Phi_3(x, t) = \frac{-igH_i}{2\omega} \varphi_3(x) \exp(-i\omega t). \quad (68)$$

Therefore, eq. (67) for the non-dimensional wave height $\varphi_3(x)$ gives

$$\frac{d}{dx} \left(gh \frac{d\varphi_3}{dx} \right) + (\omega^2 + iD_b\omega) \varphi_3 = 0, \quad (69)$$

or

$$\frac{d^2 \varphi_3}{dx^2} + (gh)^{-1} \frac{d(gh)}{dx} \frac{d\varphi_3}{dx} + \left(k_3^2 + i \frac{D_b}{\sqrt{gh}} k_3 \right) \varphi_3 = 0, \quad (70)$$

where

$$k_3 = \frac{\omega}{\sqrt{gh}}. \quad (71)$$

Using the resemblance of eq. (70) to the mild-slope eq. (9), we can write

$$D_b = \sqrt{gh}\gamma. \quad (72)$$

For a plane beach, the water depth $h(x) = -\beta x$ and eq. (70) simplifies as follows:

$$\frac{d^2\varphi_3}{dx^2} + \frac{1}{x} \frac{d\varphi_3}{dx} - \frac{\delta^2}{x} \varphi_3 = 0, \quad (73)$$

in which

$$\delta^2 = \frac{\omega^2}{g\beta} \left(1 + \frac{iD_b}{\omega} \right). \quad (74)$$

Assuming that $x < 0$, after substitution of $-x = y^2$, eq. (73) takes the form of the Bessel equation (McLachlan 1964)

$$\frac{d^2\varphi_3}{dy^2} + \frac{1}{y} \frac{d\varphi_3}{dy} + 4\delta^2\varphi_3 = 0, \quad (75)$$

with the solution

$$\varphi_3(x) = AJ_0(2\delta\sqrt{-x}) + BY_0(2\delta\sqrt{-x}), \quad (76)$$

in which $J_0(x)$ and $Y_0(x)$ are zero order Bessel functions of the first and second kind respectively. As we are looking for a solution which is finite throughout Region 3, including the waterline ($x = 0$), the coefficient B should be equal to zero. Thus, eq. (76) becomes

$$\varphi_3(x) = K_T J_0 \left[\sqrt{\left(1 + \frac{iD_b}{\omega} \right) \frac{4\omega^2(-x)}{g\beta}} \right], \quad (77)$$

in which the transmission coefficient K_T should be defined from the matching conditions at $x = -x_p$. Thus, the potential $\Phi_3(x, t)$, surface elevation $\zeta(x, t)$ and flow velocity $\bar{u}(x, t)$ are

$$\Phi_3(x, t) = \frac{-igH_i}{2\omega} K_T J_0 \left[\sqrt{\left(1 + \frac{iD_b}{\omega} \right) \frac{4\omega^2(-x)}{g\beta}} \right] \exp(-i\omega t), \quad (78)$$

$$\zeta(x, t) = \Re \left\{ \frac{H_i}{2} K_T J_0 \left[\sqrt{\left(1 + \frac{iD_b}{\omega} \right) \frac{4\omega^2(-x)}{g\beta}} \right] \exp(-i\omega t) \right\}, \quad (79)$$

$$\begin{aligned} \bar{u}(x, t) = \Re \left\{ \frac{-iH_i K_T \omega}{\beta} \left(1 + \frac{iD_b}{\omega} \right) \left[\left(1 + \frac{iD_b}{\omega} \right) \frac{4\omega^2(-x)}{g\beta} \right]^{-1/2} \times \right. \\ \left. \times J_1 \left[\sqrt{\left(1 + \frac{iD_b}{\omega} \right) \frac{4\omega^2(-x)}{g\beta}} \right] \exp(-i\omega t) \right\}. \quad (80) \end{aligned}$$

4. Solution of the boundary value problem

The potentials Φ_1 , Φ_2 and Φ_3 , determined by eqs. (4), (7) and (78), contain two functions, K_R and K_T , which are still unknown. To find them we should solve eq. (9) with the matching conditions at $x = -x_1$ and $x = -x_p$. These conditions provide continuity of pressure and horizontal velocity, normal to the vertical planes separating the fluid regions.

Matching conditions at $x = -x_1$ (Region 1/Region 2):

– continuity of pressure:

$$1 + K_R = \varphi_2(-x_1), \quad (81)$$

– continuity of horizontal and depth integrated velocity:

$$ik_1(1 - K_R) = \frac{d\varphi_2(-x_1)}{dx}. \quad (82)$$

Matching conditions at $x = -x_p$ (Region 2/Region 3):

– continuity of pressure:

$$\varphi_2(-x_p) = K_T J_0 \left[\sqrt{\left(1 + \frac{iD_b}{\omega}\right) \frac{4\omega^2 |x_p|}{g\beta}} \right], \quad (83)$$

– continuity of horizontal and depth integrated velocity:

$$PK_T = \frac{d\varphi_2(-x_p)}{dx}, \quad (84)$$

in which

$$P = \frac{2\omega^2}{g\beta} \left[\frac{\tanh(k_p h_p)}{k_p h_p} \right]^{-1} \frac{\left(1 + \frac{iD_b}{\omega}\right)}{\sqrt{\left[\left(1 + \frac{iD_b}{\omega}\right) \frac{4\omega^2 |x_p|}{g\beta}\right]}} \times \\ \times J_1 \left[\sqrt{\left(1 + \frac{iD_b}{\omega}\right) \frac{4\omega^2 |x_p|}{g\beta}} \right]. \quad (85)$$

For the arbitrary bottom profile $h(x)$ in Region 2, the resulting boundary value problem can be solved numerically only. In this paper, a finite difference method has been used and the resulting system of linear equations for φ_2 was solved by Cholesky's method for a band type matrix (Haggerty 1971). Therefore, we consider eq. (9) in the form

$$\frac{d^2\varphi_2(x)}{dx^2} + D(x)\frac{d\varphi_2(x)}{dx} + E(x)\varphi_2(x) = 0, \quad (86)$$

where

$$D(x) = \frac{1}{C(x)C_g(x)} \frac{dC(x)C_g(x)}{dx} \quad (87)$$

and

$$E(x) = k_2^2(x) + i\gamma(x)k_2(x). \quad (88)$$

Approximation of the derivatives in eq. (86) by the central differences yields

$$(2 - \Delta x D_j)f_{j-1} + (-4 + 2\Delta^2 x E_j)f_j + (2 + \Delta x D_j)f_{j+1} = 0, \quad (89)$$

in which $f = \varphi_2$ and Δx is the sampling interval. The solution of eq. (89) should be found in the domain $[-x_1, -x_p]$ at n discrete points, i.e.

$$n = \frac{|x_1| - |x_p|}{\Delta x} + 1. \quad (90)$$

At the matching points, eq. (89) takes the forms

$$\underline{\text{at } x = -x_1 (j = 1)}$$

$$K_R = f_1 - 1 \quad (91)$$

and

$$[ik_1 \Delta x (2 - \Delta x D_1) + \Delta^2 x E_1 - 2]f_1 + 2f_2 = 2ik_1 \Delta x (2 - \Delta x D_1). \quad (92)$$

$$\underline{\text{at } x = -x_p (j = n)}$$

$$K_T = \frac{f_n}{J_0 \left[\sqrt{\left(1 + i \frac{D_b}{\omega}\right) \frac{4\omega^2 |x_p|}{g\beta}} \right]} \quad (93)$$

and

$$2f_{n-1} + [(2 + \Delta x D_n)\Delta x P_1 + \Delta^2 x E_n - 2]f_n = 0, \quad (94)$$

where

$$P_1 = \frac{P}{J_0 \left[\sqrt{\left(1 + i \frac{D_b}{\omega}\right) \frac{4\omega^2 |x_p|}{g\beta}} \right]}. \quad (95)$$

The dissipation factor γ due to wave breaking in eq. (88) is a function of local wave height; therefore, the set of eq. (89) should be solved in a recurrent manner, i.e. first the non-dimensional wave height φ_2 is determined for $\gamma(x) = 0$ and $\bar{\eta} = 0$, after which the new wave height is used to calculate new values γ , D_b , $\bar{\eta}$ and φ_2 .

Choosing the position of the boundary between Regions 2 and 3 is not quite arbitrary. In Region 2 waves are considered dispersive, while in Region 3 wave motion is non-dispersive. However, for large x_p , wave motion can be represented in the form of trigonometric functions. This fact provides an opportunity to match solutions in both Regions. Massel et al. (1990) suggest that the water depth at matching point ($x = -x_p$) should be

$$h \gg \frac{25g\beta^2}{\omega^2}. \quad (96)$$

5. Examples of numerical calculations

5.1. Simplified case - a plane slope connected with a horizontal bottom

5.1.1. Governing equations and numerical calculations

Prior to discussing the arbitrary bottom profile in Region 2, let us consider a simplified domain, i.e. a plane slope merging into a horizontal bottom (Fig. 3). The velocity potential $\Phi_1(x, t)$ is given by eq. (4). As $x_1 = x_p$, Region 2 vanishes and the solution for Region 1 should match the solution for Region 3 (Mazova & Pelinovsky 1982), i.e.

$$\left. \begin{aligned} 1 + K_R &= K_T J_0(\epsilon) \\ 1 - K_R &= -i K_T \sqrt{1 + i \frac{D_b}{\omega}} S J_1(\epsilon) \end{aligned} \right\}, \quad (97)$$

where

$$\epsilon = \sqrt{\left(1 + i \frac{D_b}{\omega}\right) \frac{4\omega^2 |x_p|}{g\beta}}, \quad (98)$$

and

$$S = \sqrt{\frac{\omega^2 h_1}{g \tanh^2(k_1 h_1)}} = \sqrt{\frac{k_1 h_1}{\tanh(k_1 h_1)}}. \quad (99)$$

It should be noted that for nondispersive waves $\tanh(k_1 h_1) \rightarrow k_1 h_1$ and $S \rightarrow 1$.

The solution of eqs. (97) is

$$K_T = \frac{2}{J_0(\epsilon) - i \sqrt{1 + i \frac{D_b}{\omega}} S J_1(\epsilon)} \quad (100)$$

and

$$K_R = \frac{J_0(\epsilon) + i \sqrt{1 + i \frac{D_b}{\omega}} S J_1(\epsilon)}{J_0(\epsilon) - i \sqrt{1 + i \frac{D_b}{\omega}} S J_1(\epsilon)}. \quad (101)$$

For non-breaking waves, i.e. when $D_b = 0$, the coefficients (100) and (101) simplify to the well-known formula of Keller & Keller (1964)

$$K_T = \frac{2}{\sqrt{J_0^2(\epsilon) + S^2 J_1^2(\epsilon)}} \exp(i\varphi) \quad (102)$$

and

$$K_R = \exp(2i\varphi), \quad (103)$$

in which the phase φ becomes

$$\tan \varphi = \frac{S J_1(\epsilon)}{J_0(\epsilon)}. \quad (104)$$

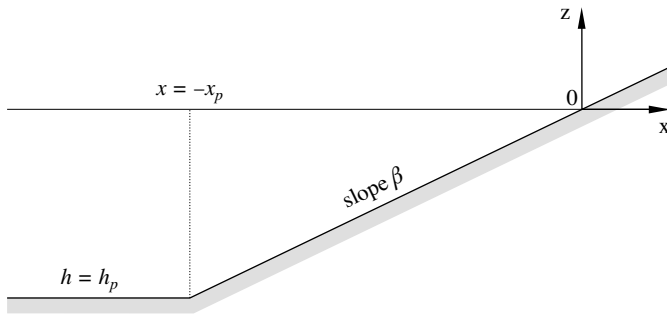


Fig. 3. Plane beach leading to a horizontal bottom

As should be expected, the reflection coefficient $|K_R| = 1$ for non-breaking waves. From eq. (79) it follows that when the set-up is neglected, the maximum height of the run-up is

$$\frac{R_{\max}}{\frac{H_i}{2}} = |K_T|. \quad (105)$$

In Figs. 4 and 5, the transmission and reflection coefficients for non-dispersive waves are shown as the function of the non-dimensional slope length x_p/L_p , in which L_p is the wavelength in Region 1. When dissipation due to breaking is neglected ($D_b = 0$), the height of the maximum run-up is about three times that of the wave height H_i for $x_p/L_p = 0.5$. The run-up height is substantially reduced for breaking waves. The reflection coefficient K_R is equal to 1 for the non-breaking waves and attenuates quickly for breaking waves, particularly on gentle slopes.

Transmission coefficient K_T and reflection coefficient K_R at $\frac{x_p}{L_p} \rightarrow 0$, correspond to the case of the vertical step which joins the deep water region ($h = h_\infty$) with a region of constant depth h (Massel 1989). Lamb (1932) showed that

$$|K_T| = \frac{2}{1 + \left(\frac{h}{h_\infty}\right)^{1/2}} \quad \text{and} \quad |K_R| = \frac{1 - \left(\frac{h}{h_\infty}\right)^{1/2}}{1 + \left(\frac{h}{h_\infty}\right)^{1/2}}. \quad (106)$$

When $h/h_\infty \rightarrow 0$, the transmission and reflection coefficients become $|K_T| = 2$ and $|K_R| = 1$ respectively.

Figs. 6 and 7 illustrate the dependence of the transmission and reflection coefficients on the dissipation factor $D_b \omega^{-1}$ for particular beach slopes. Lack of dissipation provides an unrealistically high transmission of wave energy on the beach, especially on gentle slopes, say 0.1 or 0.02. For such a situation, the similarity coefficient B_r becomes much higher than 1, which indicates that on a gentle slope, waves usually break and $D_b \neq 0$.

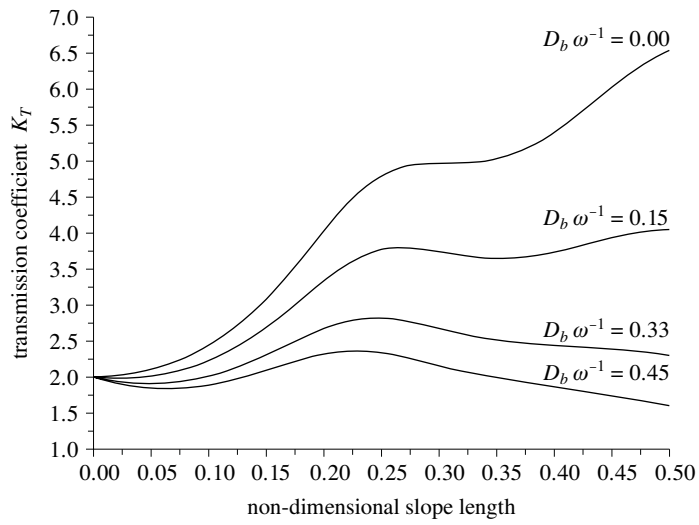


Fig. 4. Transmission coefficient as a function of non-dimensional slope length for various dissipation factors

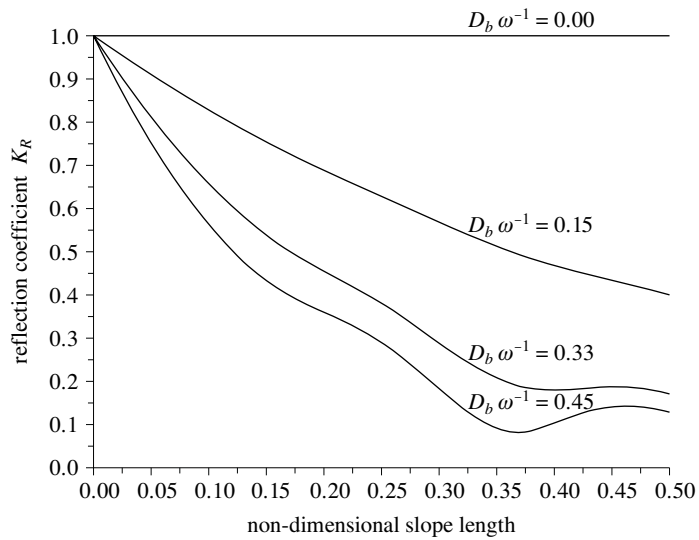


Fig. 5. Reflection coefficient as a function of non-dimensional slope length for various dissipation factors

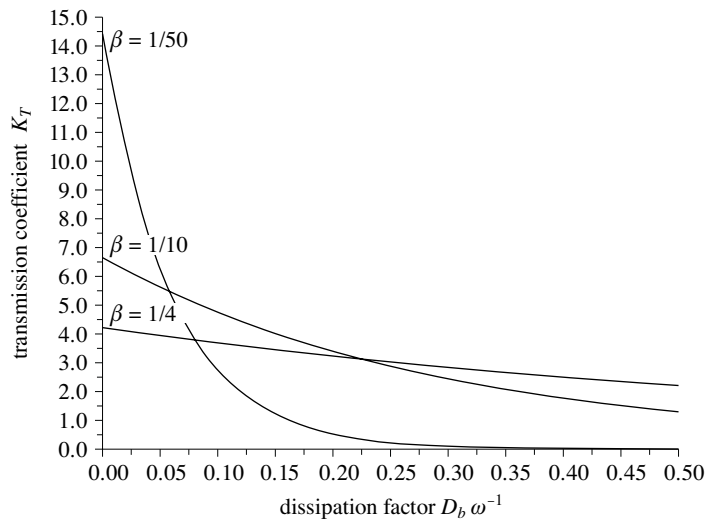


Fig. 6. Transmission coefficient as a function of the dissipation factor for various beach slopes

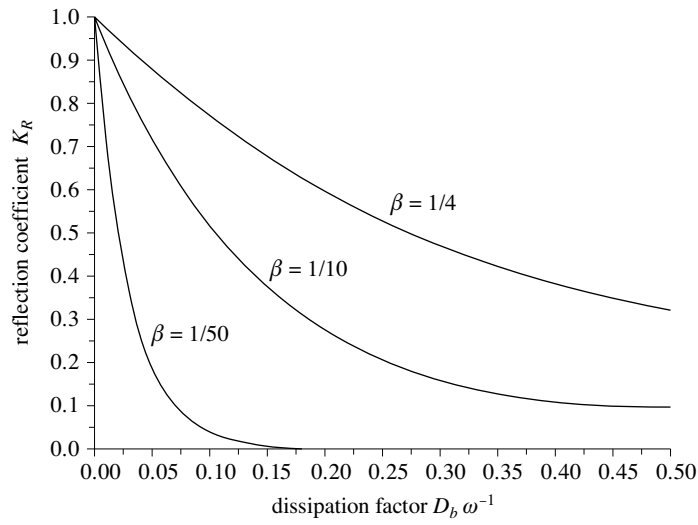


Fig. 7. Reflection coefficient as a function of the dissipation factor for various beach slopes

5.1.2. Comparison with experimental data

The experimental data on wave run-up are numerous. However, they are mostly related to long or solitary waves propagating on steep slopes, especially on marine revetments (see, for example, Titov & Synolakis (1995)). On the other hand, data on the run-up of short waves on the gentle slopes of natural beaches, which are of interest to us, are rather rare. For the purposes of this paper we used the experimental data on the run-up height reported by Saville (1958), Führböter (1985) and Gourlay (1992). They recorded only the run-up height; flow velocities were not measured. In the calculations it is assumed that the waves in Region 1 are not breaking and that the breaking process starts at some point in Region 3 and continues in this Region.

To compare the theoretical run-up height with experiments, the dissipation factor D_b due to wave breaking should be evaluated. Eqs. (14) and (72) yield the following expression for the dissipation factor D_b :

$$D_b = \sqrt{gh}\gamma = \frac{\alpha\omega}{\pi} \frac{gh}{CC_g} \left(\frac{H}{h}\right) \approx \frac{\alpha\omega}{\pi} \left(\frac{H}{h}\right), \quad (107)$$

in which α is an experimental parameter of the order one. If we determine the non-dimensional wave height $\left(\frac{H}{h}\right)$ at the breaking point, we obtain

$$\frac{D_b}{\omega} = \frac{\alpha}{\pi} \left(\frac{H}{h}\right)_{br}, \quad (108)$$

in which $\left(\frac{H}{h}\right)_{br}$ is given by eq. (16).

The Saville (1958) laboratory data of wave run-up on smooth impermeable slopes reported in the Shore Protection Manual (SPM 1984) are used for comparison. It should be noted that these data are restricted to the case when $\frac{h_p}{H_0} \approx 2$, where H_0 is the deep water wave height. Taking into account restriction (96), the calibration is valid only for slopes satisfying the relationship

$$\beta < \sqrt{\frac{8\pi^2}{25} \left(\frac{H_0}{gT^2}\right)}. \quad (109)$$

The non-dimensional deep water wave heights $\left(\frac{H_0}{gT^2}\right)$ of the experimental data are in the range 0.0003–0.0124. The corresponding range of beach slopes when the theory is applicable, for $\frac{h_p}{H_0} \sim 2$, is given in Fig. 8.

It should be stressed that the experimental values of the run-up includes the set-up mechanism. To estimate the set-up height close to the

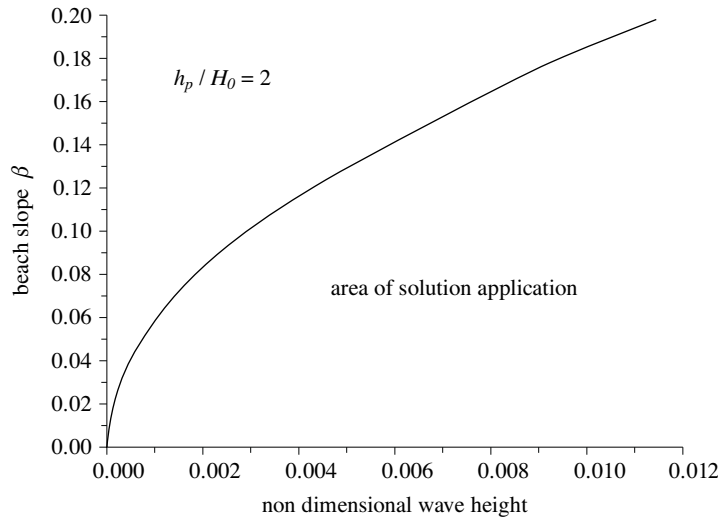


Fig. 8. Limiting beach slope (eq. 109) as a function of non-dimensional wave height for the present solution to be applicable

waterline we apply the shallow water approximation for eq. (2). Under this approximation, the set-up value $\bar{\eta}$ becomes (Massel 1989)

$$\bar{\eta}(x) = \bar{\eta}_{br} + \frac{3}{8}\gamma_{br}^2 \left(1 + \frac{3}{8}\gamma_{br}^2\right)^{-1} [h_{br} - h(x)], \quad (110)$$

in which $\gamma_{br} = \left(\frac{H}{h}\right)_{br}$ and the set-down value $\bar{\eta}_{br} = -\frac{1}{16}\gamma_{br}^2 H_{br}$. For the maximum set-up at the waterline ($x = 0$), eq. (110) gives

$$\bar{\eta}_{\max} = \bar{\eta}_{br} + \frac{3}{8}\gamma_{br}^2 \left(1 + \frac{3}{8}\gamma_{br}^2\right)^{-1} h_{br}. \quad (111)$$

Therefore, the final maximum run-up value becomes

$$R_{\max} = \frac{H_i}{2}|K_T| + \bar{\eta}_{\max} \quad (112)$$

and

$$\frac{R_{\max}}{H_0} = \frac{H_i}{2H_0}|K_T| + \frac{\bar{\eta}_{\max}}{H_0} \quad (113)$$

Using the least squares procedure, the best values for the coefficient α , which determines the minimum error between theoretical and experimental values of the maximum run-up, were calculated. In particular, for $0.0023 < \frac{H_0}{gT^2} < 0.0124$ and $\frac{1}{14} < \beta < \frac{1}{6}$ when $h_p = 2H_0$, the coefficient α is in the narrow range (1.21–1.44), while for the corresponding non-dimensional dissipation factor $\frac{D_b}{\omega}$ this range is (0.35–0.42). In order to check the strength of the dependence of the run-up height on the value of coefficient α , we assume

a constant value of $\alpha = 1.30$. The comparison between experimental and theoretical values of $\frac{R_{\max}}{H_0}$ is given in Fig. 9 for $0.0023 < \frac{H_0}{gT^2} < 0.0124$ and $\frac{1}{14} < \beta < \frac{1}{6}$, when $h_p = 2H_0$ and $\alpha = \text{const} = 1.3$. Using this value in eq. (108) we get the following parameterisation of the dissipation factor in terms of wave height at the point of onset of breaking:

$$\frac{D_b}{\omega} = \frac{1.3}{\pi} \left(\frac{H}{h} \right)_{br} = 0.413 \left(\frac{H}{h} \right)_{br} \quad (114)$$

for $0.0023 < \frac{H_0}{gT^2} < 0.0124$ and $\frac{1}{14} < \beta < \frac{1}{6}$, when $h_p = 2H_0$.

Gourlay (1992) reported the results of another set of laboratory observations of wave run-up on slope $\beta = 0.1$. The water depth h_p was maintained constant and equal to 0.2 m. Fifteen tests for wave periods $T = 1$ s and $T = 1.5$ s, as well as for wave heights ranging from 28 mm to 101 mm, were documented. The calculations showed that the experimental coefficient α in eq. (107) varied in the range (0.80–1.40), being in fact the function of two non-dimensional variables $\frac{H_0}{gT^2}$ and $\frac{h_p}{gT^2}$. The best agreement between experimental and theoretical run-up values was obtained for this function in the form

$$\alpha = 1.387 \left(\frac{h_p}{gT^2} \right)^{-1} \left(\frac{H_0}{gT^2} \right) + 0.65. \quad (115)$$

Experimental and theoretical values of $\frac{R_{\max}}{H_0}$ agree satisfactorily (Fig. 10).

Beach slopes close to the waterline are sometimes steeper than the slopes used above. Führeböter (1985) reported the results of comprehensive experiments on wave impact and wave run-up on a slope of $\beta = 0.25$, in two scales. Prototype experiments were carried out in the large wave channel (GWK) in Hannover (length 324 m, width 5 m and water depth $h_1 = 5$ m, while model experiments were made in the wave flume of water depth $h_1 = 0.5$ m. For the slope and water depths used, condition (96) puts a restriction on the number of experiments which can be applied for comparison. In particular, only runs satisfying the condition

$$T < \frac{2\pi}{5\beta} \sqrt{\frac{h_1}{g}} \quad (116)$$

can be used. Therefore, according to the above restriction, we can select only those from the list of Führeböter's experimental runs when $T < 3.59$ s for $h_1 = 5$ m and $T < 1.14$ s for $h_1 = 0.5$ m (a total of 4 runs). A comparison of the experimental results with theoretical values is given in Fig. 11.

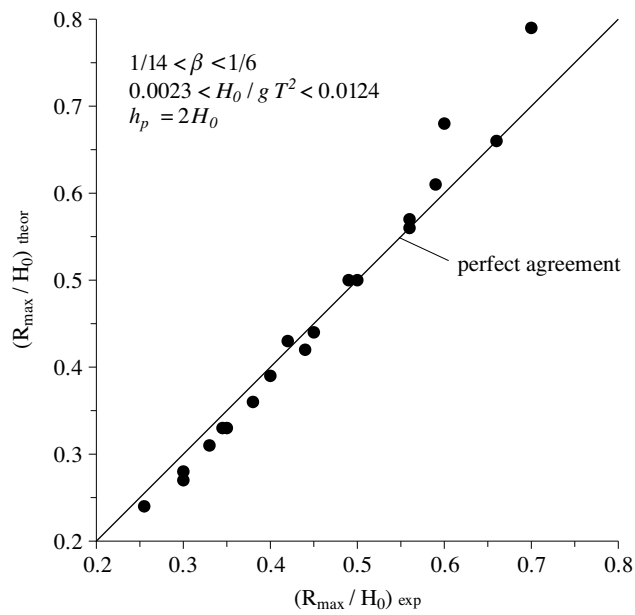


Fig. 9. Comparison of theoretical maximum run-up heights with experimental data (Saville 1958) for slopes $0.071 < \beta < 0.167$

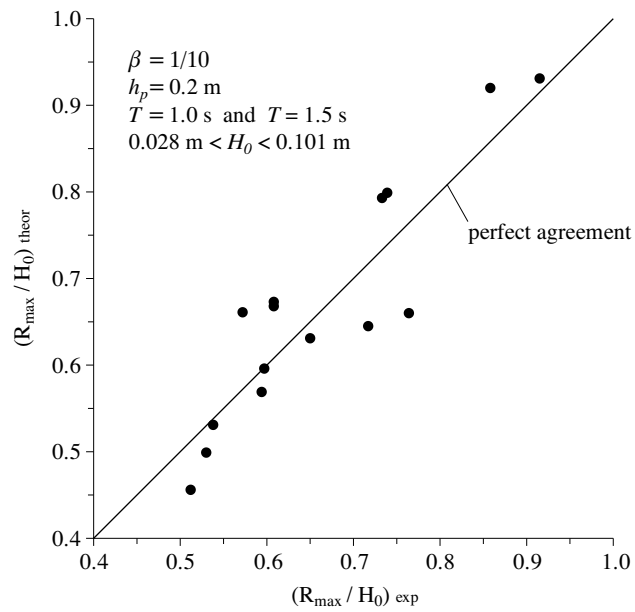


Fig. 10. Comparison of theoretical maximum run-up heights with experimental data (Gourlay 1992) for slope $\beta = 0.1$

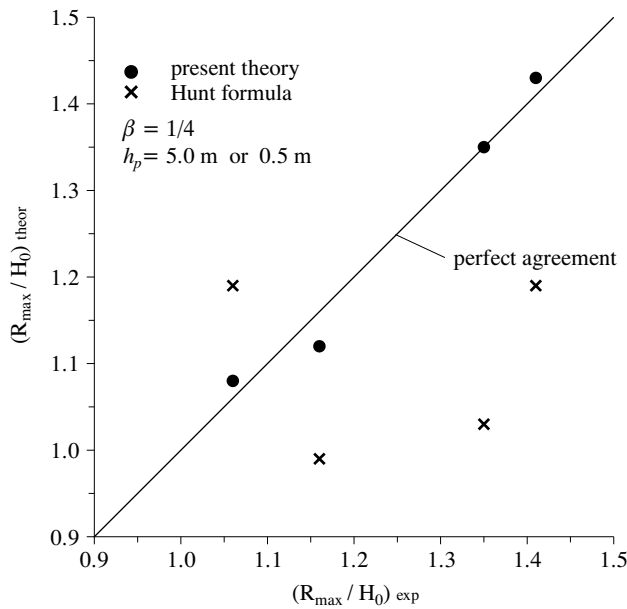


Fig. 11. Comparison of theoretical maximum run-up heights with experimental data (Führböter 1985) for slope $\beta = 0.25$

In this figure, the maximum run-up heights resulting from the well-known Hunt formula (Hunt 1959) are also given. To maintain the consistency of the comparison, the Hunt formula is rewritten as follows:

$$\frac{R_{max}}{H_0} = \frac{H_i}{H_0} \frac{\beta}{\sqrt{\frac{H_i}{L_0}}}. \quad (117)$$

This comparison indicates that the proposed theoretical solution agrees better with the experimental data than Hunt's formula does. It should be pointed out that for the beach slope of $\beta = 0.25$, the coefficient $\alpha = 0.48$ has been used to provide the best agreement with experiments. However, the available data are not sufficient for an evaluation of the more general dependence of the type $\alpha = f(\frac{H_0}{gT^2}, \beta)$.

5.2 The arbitrary bottom profile in Region 2

Unfortunately, experimental data on run-up on a beach of arbitrary profile are very rare. For the purpose of this study we apply the Saville (1958) data on wave run-up on a beach slope β , fronted by another slope 0.1, reported in the Shore Protection Manual (1984). However, these data are restricted to the case when $\frac{h_p}{H_0} = 0.80$. Using the additional condition (96), it can be found that only the runs satisfying the condition

$$\beta < \sqrt{\frac{3.2\pi^2}{25} \left(\frac{H_0}{gT^2} \right)} \quad (118)$$

can be used. We assume that the slope β is greater than 0.1. Using the value $\frac{H_0}{gT^2} = 0.0124$ (the highest value used by Saville), the only slope satisfying condition (118) is $\beta = 0.125$. When we assume that the deep water wave height $H_0 = 2$ m, the corresponding water depth $h_p = 1.6$ m, wave period $T = 4.05$ m and distances $x_1 = -112.8$ m and $x_p = -12.8$ m are used in the calculations.

In Fig. 12a, the evolution of wave amplitude over the beach bottom is shown. The observed oscillations are the result of the partial reflection of the approaching waves. The reflection coefficient K_R and the transmission coefficient K_T (from Region 2 to Region 3) are equal to 0.07 and 0.521 respectively. The slow attenuation of the wave amplitude over the slope $\beta = 0.10$ is the result of wave transformation over the beach slope. At a distance of about 28 m from waterline, wave breaking starts and the wave energy decreases substantially; however, close to the waterline the wave amplitude increases again rapidly. At the waterline ($x = 0$), the wave amplitude reaches the level of 0.51 m above SWL.

In the same figure, the corresponding wave set-up is given. Before the breaking point, the wave height changes a little and the resulting wave set-up is very small. However, from the breaking point, the wave set-up increases substantially. The set-up height $\bar{\eta}(x)$ in Region 2 ($-x_1 < x < -x_p$) was calculated using eqs. (22) and (89) in a recurrent manner. In Region 3 ($-x_p < x < 0$), the approximate formula (110) was used. Assuming that the value of $\bar{\zeta}_p$ at $x = -x_p$ is known, we obtain

$$\bar{\eta}(x) = \bar{\eta}_p + \frac{3}{8}\gamma_{br}^2 \left(1 + \frac{3}{8}\gamma_{br}^2 \right)^{-1} [h_p - h(x)], \quad (119)$$

in which $\gamma_{br} = \left(\frac{H}{h} \right)_{br}$ has been defined at the point of breaking onset at $x \sim -28$ m. It should be noted that according to formula (119), the set-up height is a linear function of x .

Fig. 12 is supplemented by Fig. 13 in which the wave amplitude and set-up within the beach segment close to the waterline is enlarged. Line 3 in this figure represents the possible maximum sea level, being a summation of the run-up amplitude (line 1) and mean sea level rise due to set-up (line 2). In particular, point A denotes the maximum wave run-up height at the waterline. Using the equivalence of the maximum characteristics of wave run-up resulting from the linear and non-linear theory discussed in Section 3.3, we can find the maximum wave run-up on the beach slope – see point B. The height of point B is the same as the height of point A, i.e. 0.89 m. It should be noted that this equivalence, in the case of breaking

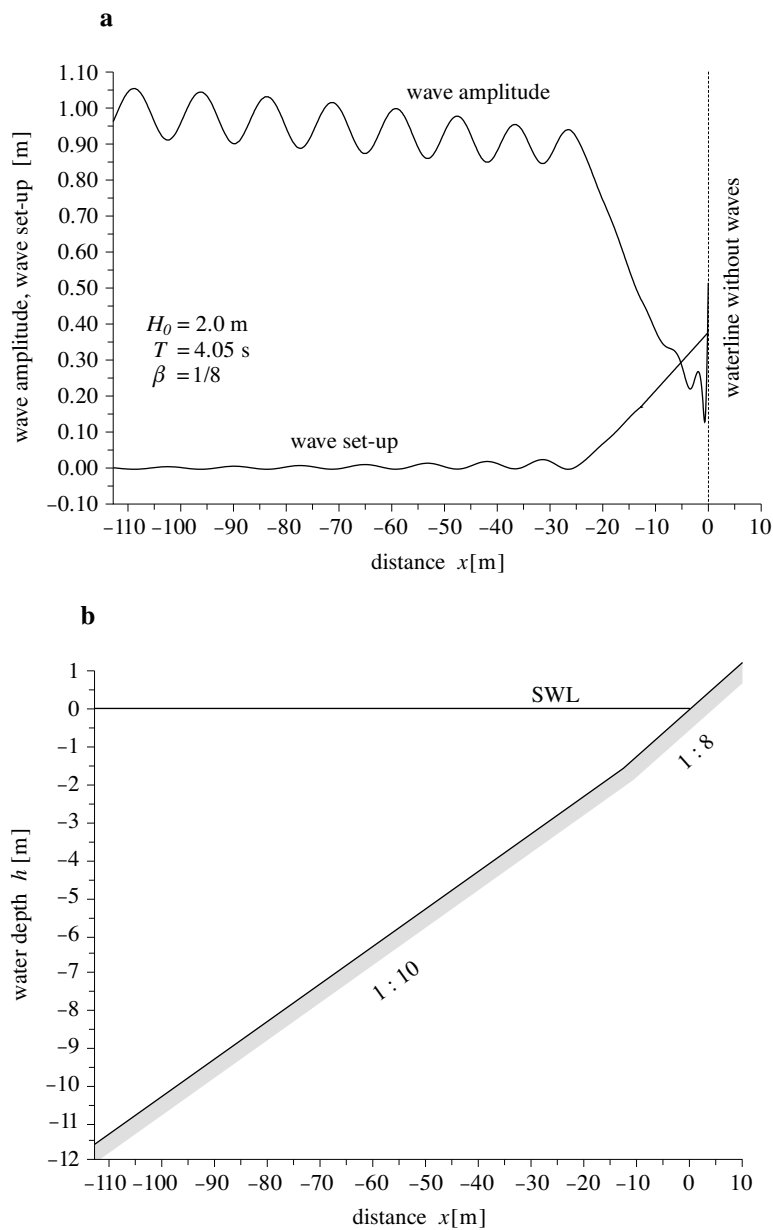


Fig. 12. Run-up of waves on a beach (two plane segments of slopes 1:10 and 1:8): variation of wave amplitude and set-up (a), beach geometry (b)

waves, can be treated only as an approximation of the unknown non-linear solution for the run-up of breaking waves. For comparison, the experimental run-up height given by Saville (1958) is shown in the figure. This value is

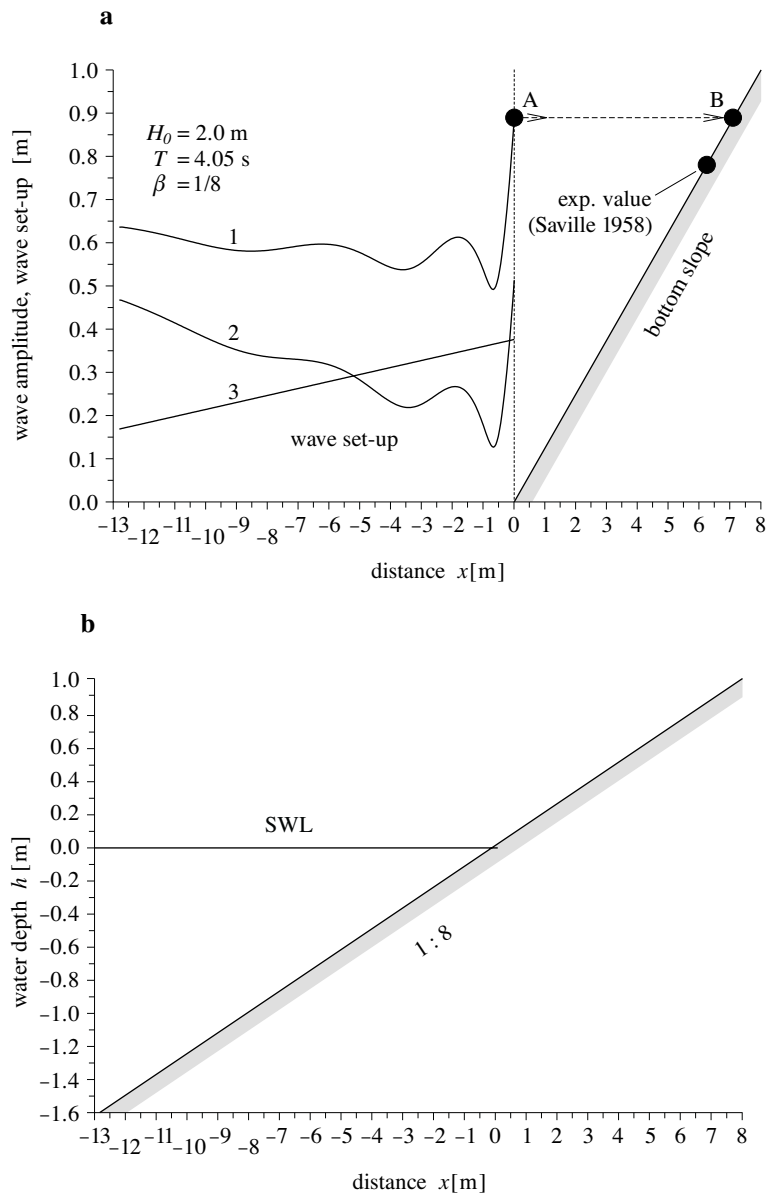


Fig. 13. Enlargement of shoreline beach segment from Fig. 12: 1 – wave amplitude, 2 – set-up height, 3 – total maximum sea level

about 12% smaller than the theoretical one. The probable reasons for the observed discrepancy are the neglect of the bottom friction in the theoretical model and the approximations used in the parameterisation of breaking waves on the beach slope.

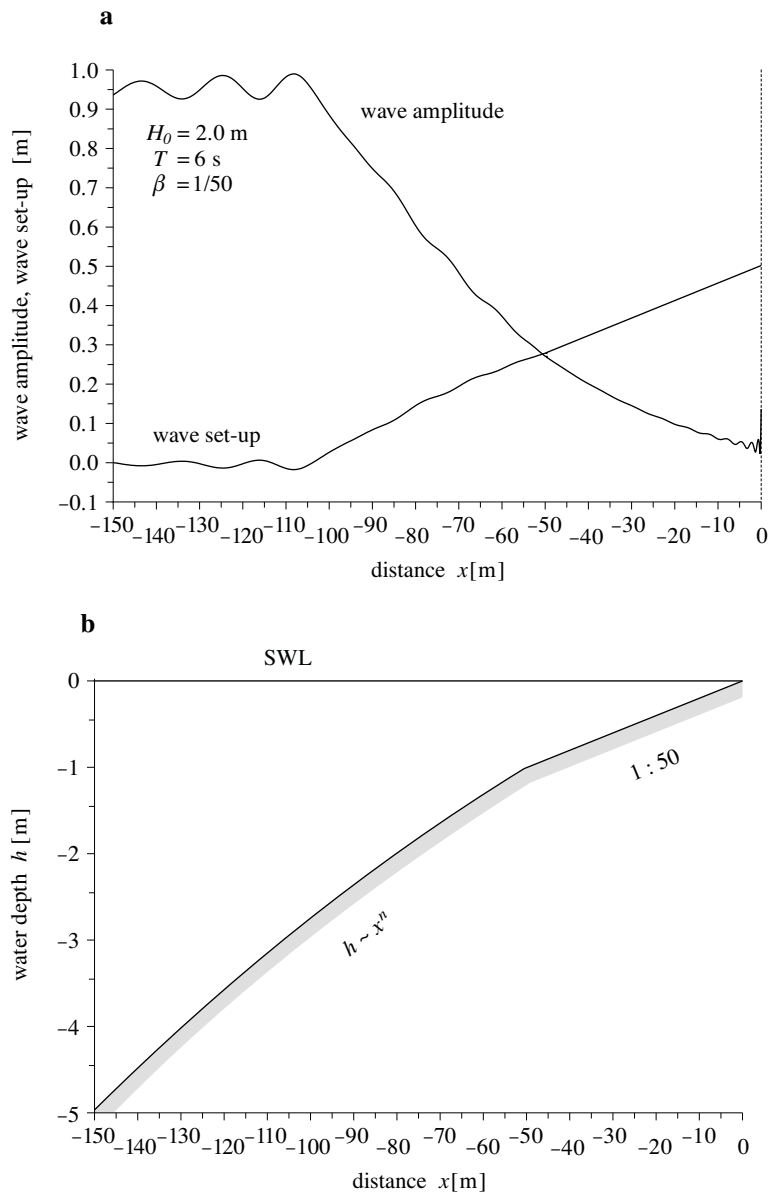


Fig. 14. Run-up of waves on a beach (very gentle plane 1:50 connected with a curved profile): variation of wave amplitude and set-up (a), beach geometry (b)

In Fig. 14, a gentle slope 0.02 is considered. Seaward of 1 m water depth, the bottom profile is given by the formula

$$h(x) = 0.0033(-x)^{1.46}. \quad (120)$$

As is shown in Fig. 14a, the breaking process starts about 110 m from the

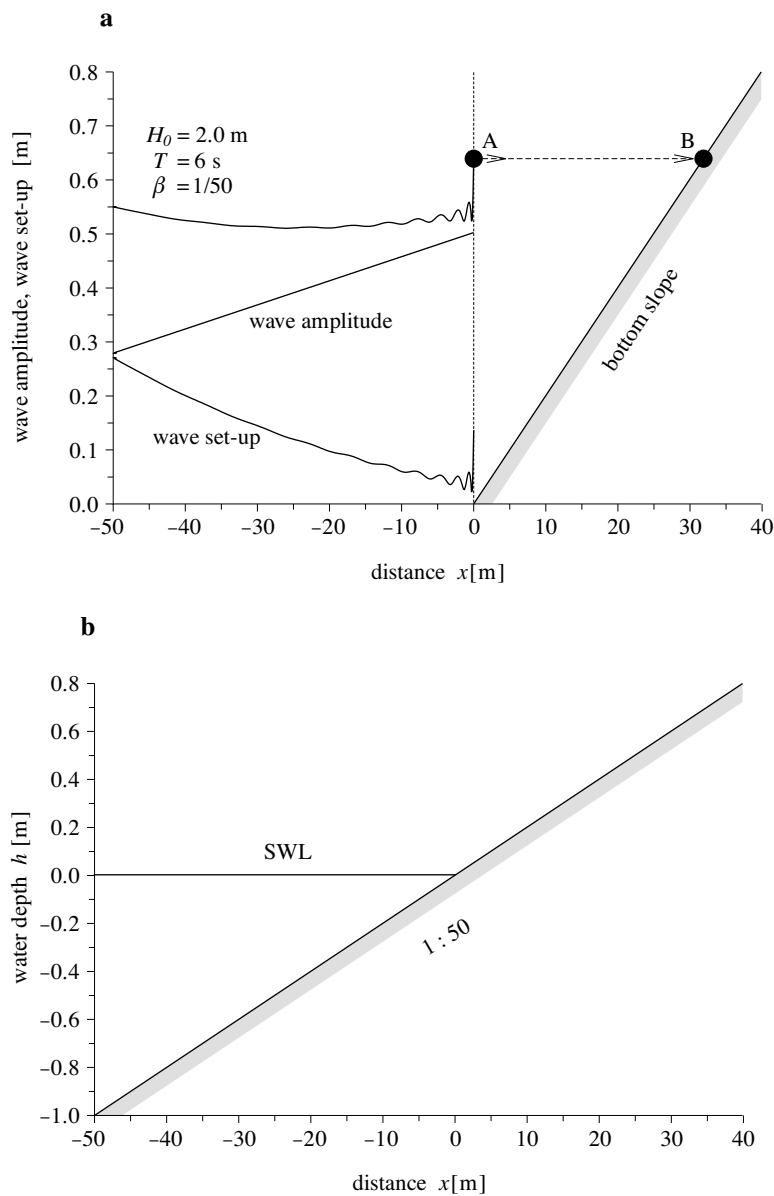


Fig. 15. Enlargement of the shoreline beach segment from Fig. 14: 1 – wave amplitude, 2 – set-up height, 3 – total maximum sea level

waterline. From this point the set-up is rising. The maximum run-up height is about 0.15 m while the set-up height is of the order of 0.50 m. Thus, the resulting total sea level at the waterline is about 0.65 m. The details of the water level in the vicinity of the waterline are shown in Fig. 15.

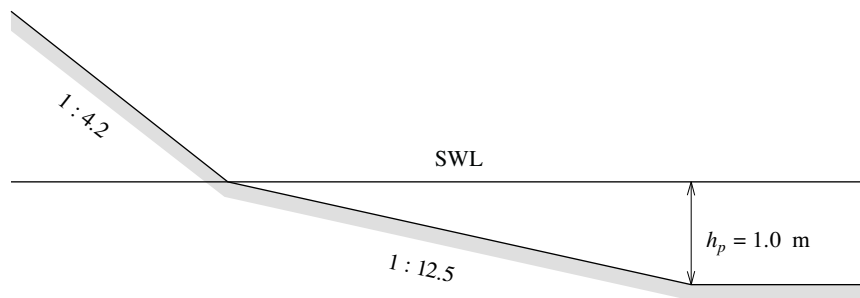


Fig. 16. Schematic representation of the sea bottom along the Hel Peninsula

Finally, we made some visual observations on the run-up on the Hel Peninsula coast in the southern Baltic, where the bottom profile can be approximated by two slopes intersecting at the still water level (see Fig. 16). At some distance the water depth was approximately constant and $h_p \sim 1$ m. The observations during moderate wind showed that the wave height H_p at water depth h_p was about 0.4 m and period $T \sim 4$ s. Using these initial values, the calculations give the set-up $\bar{\eta} = 0.13$ m at $x = 0$ and the maximum total run-up $R_{\max} = 0.62$ m. Therefore, the maximum wave extent on the beach is about 2.6 m. In fact such quantities have been observed. The sandy beaches on the Hel Peninsula were also selected for the next stage of investigations. The permeability of the beach will be considered and the groundwater circulation due to wave motion will be discussed (paper in preparation).

6. Conclusions

The following major conclusions can be drawn from this study:

1. The wave run-up on a beach face is one of the basic factors that determines beach stability and sediment transport, induces beach groundwater flow and raises the groundwater table. In the paper, the run-up mechanisms have been studied using mathematical models. In contrast to the available models, waves approaching the shoreline are assumed to be dispersive and breaking.
2. The equivalence of the non-linear and linear solutions for the extreme characteristics of the wave run-up, such as the height of maximum run-up and velocity of run-up, is used. Basically this equivalence is justified for the run-up of non-breaking waves. However, in the calculations, the equivalence was extended to breaking waves.
3. The system of equations for the run-up of breaking waves is based on the application of the mild-slope equation in deeper areas, where waves

are dispersive. The linear equations of shallow water are applied close to the shoreline, where the water depth is a linear function of distance. The dissipation factor due to wave breaking in the shallow water equation has been determined using its resemblance to the mild-slope equation for a non-permeable sea bottom.

4. The applicability of this model has been demonstrated by the comparison with the experimental data reported by Saville (1958), Führböter (1985) and Gourlay (1992). Comparison of predicted and observed wave run-up heights showed good agreement.
5. Although these findings were obtained for relatively simple beaches, they also have implications for other beach slopes. The details of the run-up given in the paper will assist future studies on infiltration in the beach body as a result of wave run-up.

References

- Abramowitz M., Stegun I. A., 1975, *Handbook of mathematical functions*, Dover Publ. Inc., New York, 1055 pp.
- Athanassoulis G. A., Belibassakis K. A., 1999, *A consistent coupled-mode theory for the propagation of small-amplitude water waves over variable bathymetry regions*, J. Fluid Mech., 389, 275–301.
- Battjes J. A., 1974, *Computation of set-up, longshore currents, run-up and overtopping due to wind-generated waves*, Comm. Hydraul., Delft Univ. Technol., Rep. 74 (2), 244 pp.
- Battjes J. A., Janssen J. P. F. M., 1978, *Energy loss and set-up due to breaking of random waves*, Proc. 16th Coast. Eng. Conf., Hamburg, 1, 563–587.
- Berkhoff J. C. W., 1973, *Computation of combined refraction-diffraction*, Proc. 13th Coast. Eng. Conf., Vancouver, 1, 471–490.
- Carrier, G. F., 1966, *Gravity waves on water of variable depth*, J. Fluid Mech., 24, 641–659.
- Carrier G. F. & Greenspan H. P., 1958, *Water waves of finite amplitude on a sloping beach*, J. Fluid Mech., 4, 97–109.
- Dingemans M. W., 1997, *Water wave propagation over uneven bottoms. Part 1. Linear wave propagation*, World Sci. Publ., Singapore, 471 pp.
- Führböter A., 1984, *Model and prototype tests for wave impact and run-up on a uniform slope 1:4*, Proc. Conf. Water Wave Res., Theory, Lab. Field, Hannover, 1–51.
- Gourlay M. R., 1992, *Wave set-up, wave run-up and beach water table: Interaction between surf zone hydraulics and groundwater hydraulics*, Coast. Eng., 17, 93–144.
- Haggerty G. B., 1972, *Elementary numerical analysis with programming*, Allyn & Bacon, Boston, 476 pp.

- Hunt J. A., 1959, *Design of seawalls and breakwaters*, J. Waterway, Port, Coast. Ocean Eng., 85, 123–152.
- Kaystrenko V. M., Pelinovsky E. N., Simonov K. V., 1985, *The run-up and transformation of tsunami in shallow water*, Sov. Meteor. Hydrol., 10, 56–62.
- Kang H. Y., Nielsen P., 1996, *Watertable dynamics in coastal areas*, Proc. Coast. Eng. Conf., 3, 4601–4612.
- Keller J. B., Keller H. B., 1964, *Water run-up on a beach*, Serv. Bureau Corp. Res., Rep. prep. for Office Naval Res., Washington.
- Kobayashi N., Greenwald J. H., 1986, *Prediction of wave run-up and riprap stability*, Proc. 20th Coast. Eng. Conf., ASCE, 3, 1958–1971.
- Lamb H., 1932, *Hydrodynamics*, Dover Publ., New York, 738 pp.
- Le Mehaute B., Koh, R. C. Y., Hwang L., 1968, *A synthesis on wave runup*, Proc. Waterway Harbor Div., 94, 77–92.
- Li L., Barry D. A., 2000, *Wave-induced beach groundwater flow*, Adv. Water Res., 23, 325–337.
- Longuet-Higgins M. S., 1983, *Wave set-up, percolation and undertow in the surf zone*, Proc. R. Soc., A 390, 283–291.
- Longuet-Higgins M. S., Stewart R. W., 1964, *Radiation stress in water waves: a physical discussion with applications*, Deep Sea Res., 11, 529–562.
- Massel S. R., 1989, *Hydrodynamics of coastal zones*, Elsevier Publ., Amsterdam, 336 pp.
- Massel S. R., 1993., *Extended refraction-diffraction equations for surface waves*, Coast. Eng., 19, 97–126.
- Massel S. R., 1996, *Ocean surface waves: their physics and prediction*, World Sci., Singapore–New Jersey, 491 pp.
- Massel S. R., 1999, *Fluid mechanics for marine ecologists*, Springer Verlag, Heidelberg–Berlin, 566 pp.
- Massel S. R., Belberova D. Z., 1990, *Parameterization of the dissipation mechanisms in the surface waves induced by wind*, Arch. Mech., 42, 515–530.
- Massel S. R., Gourlay M. R., 2000, *On the modelling of wave breaking and set-up on coral reefs*, Coast. Eng., 39, 1–27.
- Massel S. R., Pelinovsky E. N., Chybicki W., 1990, *Run-up of dispersive waves on plane beach. In oscillations and waves in liquid and gas*, Tech. Univ., Gorkiy, 6–19, (in Russian).
- Mazova R. K., Pelinovsky E. N., 1982, *Linear theory of run-up of tsunami on a beach*, Izv., Atm. Ocean Phys., 18, 124–128.
- McLachlan N. W., 1964, *Bessel functions for engineers*, PWN, Warszawa, 331 pp., (Polish edn.).
- McLachlan A., 1989, *Water filtration by dissipative beaches*, Limnol. Oceanogr., 34, 774–780.
- Pelinovsky E. N., 1982, *Nonlinear dynamics of tsunami*, Inst. Appl. Phys., Gorkiy, 226 pp., (in Russian).

- Pelinovsky E., Mazova R., 1992, *Exact analytical solutions of nonlinear problems of tsunami wave run-up on slopes with different profiles*, Natur. Hazards, 6, 227–249.
- Savage R. P., 1958, *Wave runup on roughened and permeable slopes*, J. Waterway Harbour Div., ASCE, 84, 1–38.
- Saville T., 1958, *Wave runup on composite slopes*, Proc. 6th Coast. Eng. Conf., ASCE, 691–699.
- Shore Protection Manual (SPM), 1984, Dept. Army, U.S. Army Corps Eng., Washington, I–III.
- Short A. D., 1991, *Macro-mezo tidal beach morphodynamics – an overview*, J. Coast. Res., 7, 417–436.
- Singamsetti S. R., Wind H. G., 1980, *Breaking waves: characteristics of shoaling and breaking periodic waves normally incident to plane beaches of constant slope* Delft Hydraul., Rep. M1371, 80 pp.
- Titov V. V., Synolakis C. E., 1995, *Modeling of breaking and nonbreaking long-wave evolution and run-up using VTSC-2*, Proc. ASCE, J. Waterway, Port, Coast. Ocean Eng., 121, 308–316.
- Turner I. L., 1995, *Simulating the influence of groundwater seepage on sediment transported by the sweep of the swash zone across macro-tidal beaches*, Mar. Geol., 125, 153–174.
- Voltzinger N. E., Klevanny K. A., Pelinovsky E. N., 1989, *Long wave dynamics of the coastal zone*, Gidrometeoizdat, 271 pp., (in Russian).
- Walton T. L., Ahrens J., 1989, *Maximum periodic wave run-up on smooth slopes*, J. Waterway, Port, Coast. Ocean Eng., 115, 703–708.
- Węśławski J. M., Malinga B., Kotwicki L., Opaliński K., Szymelfenig M., Dutkowski M., 2001, *Sandy coastlines – are there conflicts between recreation and natural values?*, Oceanol. Stud., (in press).